We are IntechOpen, the world's leading publisher of Open Access books Built by scientists, for scientists

6,900
Open access books available

186,000
International authors and editors

200M
Downloads

Our authors are among the

154
Countries delivered to

TOP 1%
most cited scientists

12.2%
Contributors from top 500 universities

WEB OF SCIENCE™

Selection of our books indexed in the Book Citation Index
in Web of Science™ Core Collection (BKCI)

Interested in publishing with us?
Contact book.department@intechopen.com

Numbers displayed above are based on latest data collected.
For more information visit www.intechopen.com

Thermophysical Properties and SANS Studies of Nanoemulsion Heat Transfer Fluids

Bao Yang and Jiajun Xu

Additional information is available at the end of the chapter

Abstract

Cooling is one of the most important technique challenges faced by a range of diverse in-dustries and military needs. There is an urgent need for innovative heat transfer fluids with improved thermal properties over currently available ones. This chapter discusses the development and characterization of nanoemulsion heat transfer fluids with phase changeable nanodroplets to increase the thermophysical properties and the heat transfer rate of the fluid. Nanoemulsion heat transfer fluids can be formed by dispersing one fluid into another immiscible fluid as nanosized structures such as droplets and tubes, in which those nanostructures are swollen reverse micelles with the dispersed phase and stabilized by the surfactant molecules. In addition to the enhancement of thermophysical properties such as thermal conductivity by mixing another liquid of higher thermal con-ductivity, an even larger amount of heat can be absorbed or released when these nano-droplets undergo phase transition from liquid to gas or vice versa, and thus enhancing the heat transfer rate. Three types of nanoemulsion heat transfer fluids are introduced: al-cohol-in-polyalphaolefin, water-in-FC-72, and water-in-polyalphaolefin. Structural and property characterizations of these nanoemulsion heat-transfer fluids are the two main aspects of this chapter. This chapter also identifies several critical issues in the nanoemul-sion heat transfer fluids to be solved in the future.

Keywords: Nanoemulsion, Thermophysical Property, Heat Transfer, Small Angle Neu-tron Scattering (SANS)

1. Introduction

Cooling is one of the most important technical challenges faced by a range of diverse industries: microelectronics, optoelectronics, and, especially, power electronics [1–8]. This technology gap is the result of the higher currents, switching frequencies, and component densities of today's electronics and power electronics. The advances in semiconductor materials and more precise

fabrication techniques have the unfortunate side effect of generating higher amounts of waste heat within a smaller volume. Today, it is not unusual to see heat fluxes of 200 W/cm^2 in a power module, a figure that is expected to increase over 1000 W/cm^2 in the near future.

Thermal management of such high flux is becoming the bottleneck to improvements in electronics and power electronics. Existing cooling systems is striving to meet the ever-increasing demand in higher computational power and smaller footprint. It is important that a cooling system with significantly improved heat transfer systems and their kernel components can be developed; in particular the cooling fluid used inside many heat transfer systems but yet has received little attention. The heat transfer fluids used in these heat transfer systems, including the coolants, lubricants, oils, and other fluids, limit the capacity and compactness of the heat exchangers that use these fluids due to their inherently poor heat transfer properties. The heat transfer capability of the heat exchangers can be easily amplified if fluids with better thermal properties are used. Therefore, development of innovative heat transfer fluids with improved thermal properties over those currently available is urgently needed.

The strategy of adding solid, highly conductive particles to improve thermal conductivity of fluids has been pursued since Maxwell's theoretical work was first published more than 100 years ago [9]. Early-stage studies have been confined to millimeter- or micrometer-sized solid particles dispersed in fluids. In the past decade, researchers have focused on suspensions of nanometer-sized solid particles, known as nanofluids [2, 8]. Many reviews and introductory reports on nanofluids have already been published [1, 2, 4, 10–14].

In this paper, it is intended to introduce some recent developments in another type of engineered heat transfer fluids, in which phase changeable nanodroplets are added to increase the thermophysical properties and heat transfer rate of the base fluids [15–22]. This chapter starts with the introduction of nanoemulsion fluids with potential application in thermal fluids. It is followed by the discussion on structural and thermophysical characterization techniques for nanoemulsion fluids [15–19, 21]. Then, three groups of nanoemulsion fluids and their properties are discussed. This chapter is not intended to serve as a complete description of all nanoemulsion fluids available for heat transfer applications. The selection of the coverage was influenced by the research focus of the authors and reflects their assessment of the field.

2. Nanoemulsion heat transfer fluids

One fluid is dispersed into another immiscible fluid as nanosized structures such as droplets and tubes to create a "nanoemulsion fluid." Those nanosized structures of the dispersed phase are micelles stabilized by the surfactant molecules on the outside. Nanoemulsion fluids are part of a broad class of multiphase colloidal dispersions [15–19, 21]. Different from the preparation of the nanofluids and emulsions [23–31], the nanoemulsion fluids are spontaneously generated by self-assembly which does not require external shear force. Thus the nanoemulsion fluids are thermodynamically stable [16–19, 23, 32–44]. Table 1 is the comparison between self-assembled nanoemulsion fluids and conventional emulsions. Nanoemulsion fluids made of specific fluids are suited for thermal management applications. Figure 1 shows

a picture of ethanol-in-polyalphaolefin (PAO) nanoemulsion heat transfer fluids: both PAO and PAO-based nanoemulsion fluids are transparent but the nanoemulsion exhibits the Tyndall effect [15, 16, 19, 21, 45, 46].
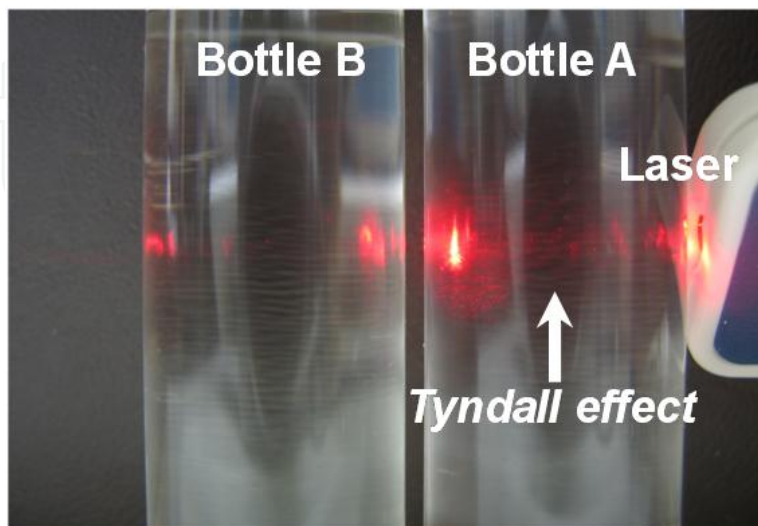
Figure 1. Pictures of ethanol-in-PAO nanoemulsion fluids (Bottle A) and pure PAO (Bottle B). Liquids in both bottles are transparent. The Tyndall effect (i.e., a light beam can be seen when viewed from the side) can be observed only in Bottle A when a laser beam is passed through Bottles A and B.

Sample	Property	Nanoemulsion	Emulsion
1	Appearance	Transparent	Turbid
2	Interfacial tension	Ultra low (usually <<1 mN/m)	Low
3	Droplet size	<50 nm	>500 nm
4	Stability	Thermodynamically stable, long shelf life	Thermodynamically unstable
5	Preparation	Self-assembly	N of external shear
6	Viscosity	Newtonian	Non-Newtonian

**Table 1.** Comparison of nanoemulsion fluids and emulsions

2.1. Formation of self-assembled nanoemulsion fluids

Self-assembled nanoemulsion fluids are thermodynamically stable, and the formation of these fluids can be explained using the classical thermodynamic theory [23, 34–39, 42, 43, 47–49]. The nanoemulsion fluid consists of one oil phase, one water phase, and certain surfactants. The adding of surfactant lowers the surface tension of the oil–water interface and the change in free energy of the system is given by Equation 1,

$$DG_f = \gamma DA - T \cdot DS \tag{1}$$

where DG_f is the free energy of formation, γ is the surface tension of the oil–water interface, DA is the change in interfacial area upon nanoemulsification, DS is the change in entropy of the system, and T is the absolute temperature. The change in DA is very high due to the large number of nanosized droplets in the nanoemulsion fluids. However, the interfacial tension γ is very small (usually <<1 mN/m), and therefore the increase in the surface energy, γDA, could be smaller than the entropy arising from the mixing. The favorable entropic contributions also arise from dynamic processes such as surfactant diffusion in the interfacial layer and monomer–micelle surfactant exchange. The entropy of mixing can be large enough to compensate for the positive interfacial free energy and to give the nanoemulsion system a free energy lower than that of the unmixed components. So the self-assembled nanoemulsion fluids can be formed through self-assembly and are in fact thermodynamically stable system [23, 43, 50]. There are mainly two approaches to prepare nanoemulsion fluids: the spontaneous emulsification method (or the so-called phase titration method) and the phase-inversion method [23, 43].

Figure 2 shows the typical phase behavior diagram of a ternary system that contains two immiscible so-called oil and water phases and an amphiphilic surfactant component. The term "water" refers to a polar phase while "oil" is used for an apolar organic phase. When a system has a composition that lies in the shaded areas, a nanoemulsion fluid, either oil-in-water or water-in-oil, can be formed through self-assembly.
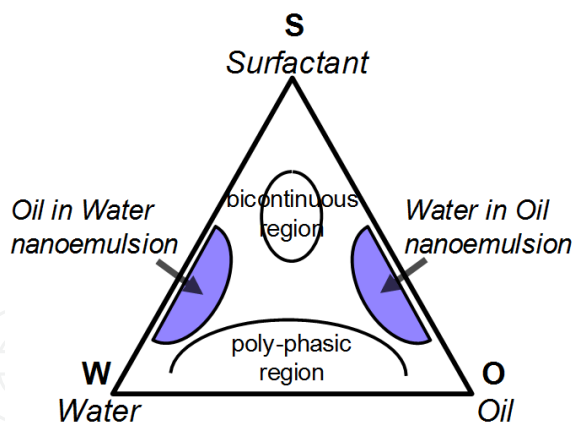
Figure 2. Schematic phase diagram of a water-oil-surfactant ternary system. The shaded areas are regions where self-assembled nanoemulsions are found.

2.2. Structure characterization methods

Similar to other multiphase colloidal dispersions, the microstructure of nanoemulsion fluids is sensitive to many factors, including the different dispersed liquid, surfactants and base fluid, and molar ratio of dispersed liquid to surfactant [34]. In addition to that, temperature, pH-value, and salinity also play an important role in the microstructure [23]. So accurate charac-

terization of the microstructure of nanoemulsion fluids is important to understand the nanoemulsion fluids and yet challenging and costly to perform. In the past, small angle X-ray scattering (SAXS), small angle neutron scattering (SANS), dynamic or laser-light scattering (DLS), transmission electron microscopy (TEM), and nuclear magnetic resonance (NMR) have been used for the structure characterization [23]. In addition, the measurement of nanoemulsion properties, such as viscosity, electric conductance, thermal conductivity, dielectric permittivity, electrophoretic birefringence, ultrasonic interferometry, and ultrasonic absorption, can also provide information on the internal microstructure.

SANS allows the characterization of the structures inside the material on the nanometer (10^{-9} m) to micrometer (10^{-6} m) scale [51]. Many advanced engineering materials obtain unique performance because of their engineered structures on this length scale. For example, the toughness of high-impact plastics depends on the admixture of stiff and flexible segments of polymer molecules on the nano-to-micro scale, as well as, many biological processes in cells: from the storage of information on magnetic disks, to the hardness of steels and superalloys, to the conduction of current in superconductors, and many other materials properties.

Among all methods currently available for characterizing the microstructure of nanoemulsion fluids, small-angle neutron scattering (SANS) provides a unique approach to probe structure in liquids thanks to the distinctive penetrating power of neutron. Unlike the conventional dynamic light-scattering method using laser or X-rays, it can be applied to "concentrated" colloidal suspensions (e.g., >1 % volume fraction) and can penetrate through a container [51–57]. Another advantage of SANS method is the deuteration method, in which deuterium labeled components in the sample in order to enhance their contrast that it can probe specific molecules or structure inside the sample with the deuteration technique. This unique method allows SANS to measure density fluctuations and composition (or concentration) fluctuations, which is very important to understand the structure inside nanoemulsion fluids [23].

2.3. Thermophysical properties characterization methods

2.3.1. Thermal conductivity

Low thermal conductivity is a primary limitation in the development of energy-efficient heat transfer fluids that are required in many industrial applications. Conventional heat transfer fluids have relatively poor thermal conductivity compared to metals [9]. It has been reported that the dispersed liquid nanodroplets could alter thermal conductivity of the base fluids [1, 2, 4, 58–61]. However, because of the absence of a theory for the thermal conductivity of nanoemulsion heat transfer fluids, an investigation of the effect of nanodroplets on the thermal conductivity will be conducted.

There are two widely used methods to measure the thermal conductivity of nanoemulsion fluids which includes (1) the transient hot-wire technique and (2) 3ω-wire method [62]. In the transient hot-wire method, thermal conductivity value is determined from the heating power and the slope of temperature change versus logarithmic time. The 3ω-wire method is used to measure the fluid thermal conductivity [19, 21, 62, 63]. This method is actually a combination of the transient hot-wire method and the 3ω-wire method, in which a metal wire is suspended

to a liquid acting as both heater and thermometer. One advantage of this 3ω-wire method is that the temperature oscillation can be kept low enough: it is usually below 1 K as compared to about 5 K for the hot-wire method. It greatly helps to retain constant liquid properties of test liquid during measurement. Calibration experiments were performed for hydrocarbon (oil), fluorocarbon, and water at atmospheric pressure before each measurement.

2.3.2. Viscosity

Viscosity is a measure of the resistance of a fluid which is being deformed by either shear stress or tensile stress. Viscosity is another macroscopically observable parameter that characterizes a nanoemulsion fluid, and it may range anywhere between a low viscous fluid and a gel state. It is an important quantity for many practical applications of nanoemulsion fluids, especially those used for hydraulic fluids. For instance, pumping such systems might be of interest in their application, and here viscosity plays an important role. Viscosity can be determined from the equation below:

$$F = \mu A \frac{u}{y} \tag{2}$$

where F is the stress force, u is the velocity, A is the area and μ is the proportionality factor called dynamic viscosity. The kinematic viscosity v is related to the dynamic viscosity by dividing by the density of the fluid, $v = \frac{\mu}{\rho}$.

Viscosity of a nanoemulsion fluid depends largely on its microstructure, that is, the type of aggregates that are present, on their interactions, and on the concentration of the system. So the viscosity can be used to monitor structural changes in the nanoemulsion system. In order to do so, one has to compare the experimental data to theoretical expressions that give the viscosity expected for certain model systems.

2.3.3. Specific heat measurement

The specific heat is the amount of heat per unit mass required to raise the temperature by one degree Celsius. A differential scanning calorimeter (DSC) is usually used to measure a material's specific heat. In DSC measurement, it compares the differential heat flow (heat/time) between the measured material and the empty reference pan by adjusting the heat flux into a pan containing the sample with the heat flux into an empty pan while keeping both the measured sample and reference sample at nearly the same temperature. The difference in the amount of heat supplied to the sample and the reference is recorded as a function of temperature (or time), and the positive or negative peaks in the relationship correspond to exothermic or endothermic reactions in the sample, respectively. In order to determine the sample heat capacity, three measurements are usually carried out: for the sample, for the baseline, and for a standard. The baseline is subtracted from the sample measurement to obtain absolute values of the heat flow to the sample. The heat capacity is to be determined by the heat flow, the temperature rise, and the sample mass.

3. Nanoemulsion heat transfer fluids

3.1. Ethanol-in-Polyalphaolefin (PAO) nanoemulsion fluids

Polyalphaolefin (PAO) has been widely used as dielectric heat transfer fluids and lubricants due to its chemical stability within a wide temperature range. However, its thermal properties are relatively poor compared to other heat transfer fluids [64]. Ethanol-in-PAO is a liquid–vapor phase change nanoemulsion fluid, in which over 90 % consist of PAO to keep its chemical stability very close to pure PAO. Meanwhile, the ethanol nanodroplets could evaporate explosively and thus enhance the heat-transfer rate of the base fluid PAO [16]. The microstructure and thermophysical properties of the ethanol-in-PAO nanoemulsion fluids are discussed below.

3.1.1. Microstructure of ethanol-in-PAO nanoemulsion fluids

The microstructure of ethanol-in-PAO nanoemulsion fluids are on the NG-3 (30 m) beamline at the NIST Center for Neutron Research (NCNR) in Gaithersburg, MD. Samples are loaded into 2-mm quartz cells. Figure 3 shows the SANS data, the scattering intensity I versus the scattering vector $q = 4\pi \sin(\theta/2)/\lambda$, where λ is the wavelength of the incident neutrons, and θ is the scattering angle. The approximation $q = 2\pi\theta/\lambda$ is used for SANS (due to the small angle θ). The analysis of the SANS data suggests that the inner cores of the swollen micelles, that is, the ethanol droplets, are spherical and have a radius of about 0.8 nm for 9 vol. %.
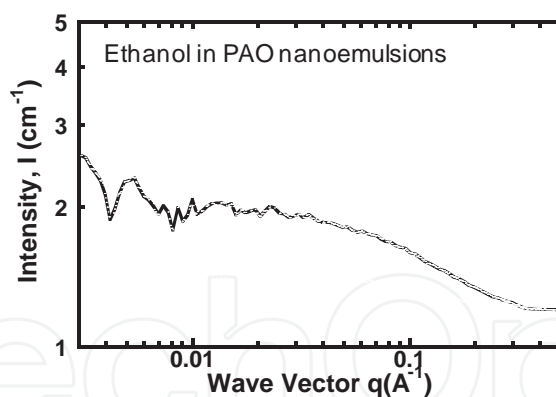
Figure 3. Intensity I vs. Wave Vector q measured in ethanol-in-PAO nanoemulsion fluids.

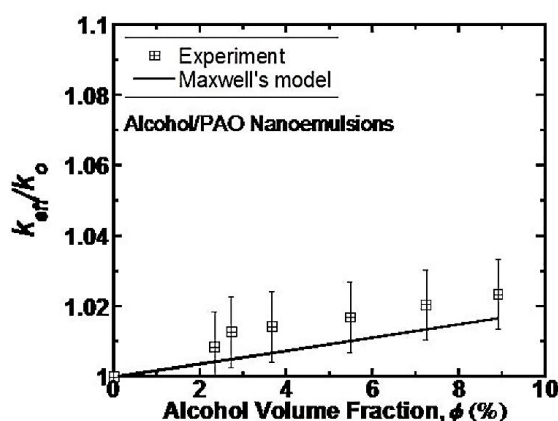### *3.1.2. Thermal conductivity of ethanol-in-PAO nanoemulsion fluids*

The relative thermal conductivity in ethanol-in-PAO nanoemulsion fluids measured using the 3ω-wire method along with the prediction by the Maxwell model (one model based on effective medium theory [EMT]) is shown in Figure 4. The relative thermal conductivity is defined as k_{eff}/k_o, where k_o and k_{eff} are thermal conductivities of the base fluid and nanoemulsion fluids, respectively. The effective medium theory reduces to Maxwell's equation for suspensions of well-dispersed, non-interacting spherical particles,

$$\frac{k_{\text{eff}}}{k_o} = \frac{k_p + 2k_o + 2\phi\left(k_p - k_o\right)}{k_p + 2k_o - \phi\left(k_p - k_o\right)} \tag{3}$$

where k_o is the thermal conductivity of the base fluid, k_p is the thermal conductivity of the particles, and ϕ is the particle volumetric fraction.

It can be seen in Figure 4 that the relative thermal conductivity of ethanol-in-PAO nanoemulsion fluids is rather moderate (e.g. 2.3 % increase for 9 vol. % ($k_{\text{PAO}} = 0.143$ W/mK and $k_{\text{alcohol}} = 0.171$ W/mK [64, 65]), and no strong effects of Brownian motion on thermal transport are experimentally found in those fluids although the nanodroplets are extremely small, around 0.8 nm [16]. The thermal conductivity also appears to be linear with the loading of ethanol nanodroplets over the loading range from 0 to 9 vol. %. The Maxwell's equation, however, underestimates the viscosity increase in the ethanol-in-PAO nanoemulsion fluids, as can be seen in Figure 4. This is probably because Maxwell's equation does not take into account the shape transformation with different ethanol concentrations. It may suggest that the ethanol droplets form column-like with high aspect ratio of length to radius, which leads to a higher thermal conductivity enhancement in nanoemulsion fluids than the spherical droplets.

Figure 4. Relative thermal conductivity of ethanol-in-PAO nanoemulsions measured at different volume fractions of ethanol nanodroplets. The estimate from Maxwell's model is shown for comparison.
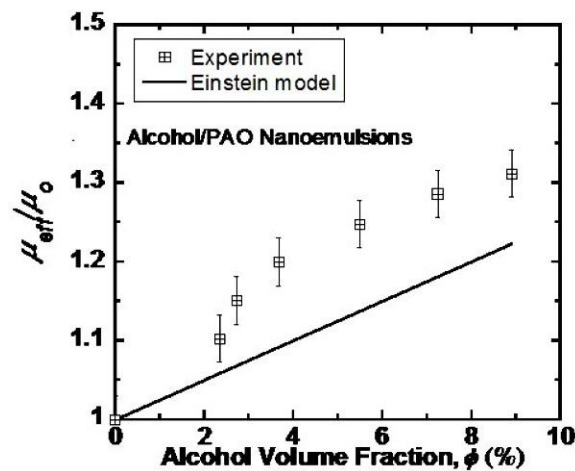
3.1.3. Viscosity of ethanol-in-PAO nanoemulsion fluids

Figure 5 shows the relative dynamic viscosity, μ_{eff}/μ_o, for the ethanol-in-PAO nanoemulsion fluids with varying alcohol loading, which is measured using a commercial viscometer (Brookfield DV-I Prime). The calibration is carried out using the pure PAO and its dynamic viscosity is found to be 7.3 cP which compares well with the literature value. Similar to thermal conductivity plotted in Figure 4, an approximately linear relationship is observed between the viscosity increase and the loading of alcohol nanodroplets in the range of 0–9 vol. %, but at a much larger percentage. For example, the measured viscosity increase is 31 % for 9 vol. %.

ethanol loading, compared to a 2.3 % increase in thermal conductivity. The viscosity increase of dilute colloids can be predicted using the Einstein equation[12],

$$\mu_{eff} / \mu_0 = 1 + 2.5\phi \tag{4}$$

where μ_{eff} is the nanoemulsion viscosity, μ_0 is the base fluid PAO viscosity and φ is the volumetric fraction of encapsulated ethanol nanodroplets. The viscosity increase in the ethanol-in-PAO nanoemulsion fluids is underestimated by the Einstein equation, as can be seen in Figure 5. This discrepancy is probably because the droplet volume fraction, ϕ, used in the viscosity calculation does not take into account the surfactant layer outside the alcohol core and Einstein equation used here is derived from dilute system.

Figure 5. Relative viscosities of ethanol-in-PAO nanoemulsions measured at different volume fractions of ethanol nanodroplets. The estimate from Einstein model is shown for comparison.
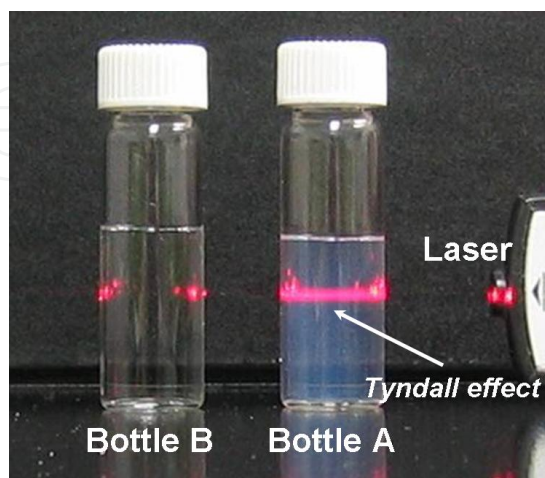
3.2. Water-in-FC-72 nanoemulsion fluids

Water-in-FC-72 nanoemulsion fluids are another group of nanoemulsion fluids designed for heat transfer purpose, in which water could undergo liquid–solid transition and thus increase heat transfer rate of the base fluid FC-72. FC-72 is one of the lines of Fluorinert™ Electronic Liquids developed by 3M™, which is used as the cooling fluids in liquid-cooled thermal management systems due to its low boiling point and excellent dielectric properties [66]. However, its heat transfer properties such as thermal conductivity and heat capacity are much inferior, compared to other fluids such as water.
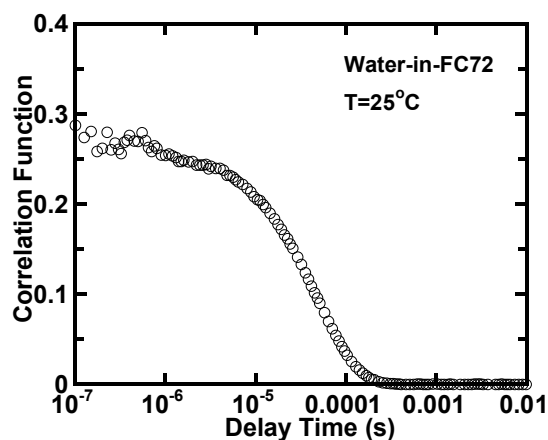
3.2.1. Microstructure of water-in-FC-72 nanoemulsion fluids

Water-in-FC-72 nanoemulsion fluids are generated by emulsifying deionized water into FC-72 with a small amount of perfluorinated amphiphiles. Figure 6 (a) shows the picture of the water-in-FC-72 nanoemulsion fluids and the pure FC-72. The autocorrelation function of the scattered

light for the 12 vol. % water-in-FC-72 nanoemulsion fluids is plotted in Figure 6 (b), in which the curve shows a typical exponential decay of the correlation function versus time [19, 21]. The Brownian diffusivity and effective hydrodynamic radius of the nanodroplets are found to be $3.5{\times}10^{-7}$ cm^2/s and 9.8 nm at $T = 25^{o}$C, respectively.

(a)

(b)

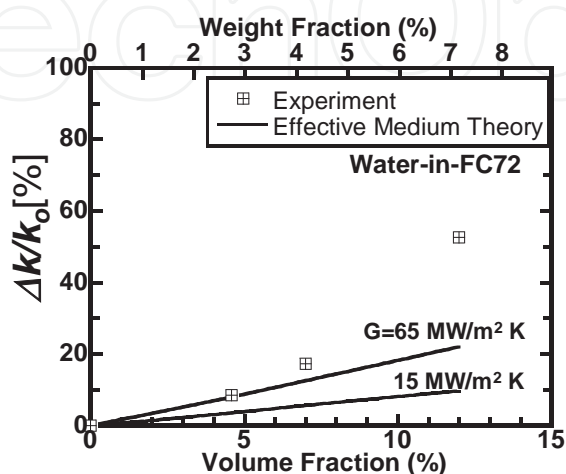**Figure 6.** (a). Pictures of Water-in-FC-72 nanoemulsion fluids (Bottle A) and pure FC-72 (Bottle B). (b). Correlation function of the scattered light for the 12 vol.% Water-in-FC-72 nanoemulsion fluids. Measurements taken by a Photocor-Complex DLS instrument.

3.2.2. Thermal conductivity of water-in-FC-72 nanoemulsion fluids

Thermal conductivity of the water-in-FC-72 nanoemulsion is measured for different water loadings, and the results are shown in Figure 7. The 3ω -wire method is used to measure the fluid thermal conductivity. In water-in-FC-72 nanoemulsion fluids, the water phase has a thermal conductivity much higher than that of the base liquid FC-72. Water's thermal conductivity is 0.609 W/(mK) at 300 K and FC-72's thermal conductivity is much smaller, about 0.066 W/mK [66]. The addition of water is expected to improve the effective thermal conductivity of FC-72.

A very large increase in thermal conductivity (up to 52 % for water-in-FC-72 nanoemulsion of 12 vol. % water) can be seen in Figure 7. The observed enhancement in thermal conductivity is much larger than that predicted by the EMT with assumption of spherical droplets [67]. This suggests that the water droplets are column-like with high aspect ratio of length to radius, which leads to a higher thermal conductivity enhancement in nanoemulsion fluids than the spherical droplets.
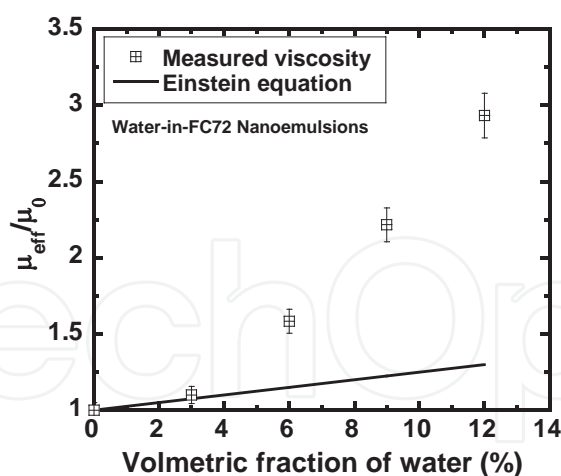

Figure 7. Relative thermal conductivity of water-in-FC-72 nanoemulsion fluids versus volume fraction of water. The estimate from EMT is shown for comparison.

3.2.3. Viscosity of water-in-FC-72 nanoemulsion fluids

The dynamic viscosity of water-in-FC-72 nanoemulsions of different nanodroplet concentrations is measured using a Brookfield viscometer at room temperature. The results have been normalized to the viscosity of pure FC-72 and are shown in Figure 8. The measured viscosity increase is nonlinear with the higher concentration of water added inside which agrees well with the nonlinear increase in thermal conductivity. This nonlinear increase in viscosity is common in colloidal systems, and has been interpreted by the aggregation of nanodroplets, that is, formation of column-like microstructure. Similar to the ethanol-in-PAO nanoemulsion fluids discussed previously, the Einstein equation significantly underpredicts the viscosity increase in the water-in-FC-72 nanoemulsion fluids at relatively high water loadings, as can be seen in Figure 8.

3.2.4. Effective heat capacity of water-in-FC-72 nanoemulsion fluids

Another significant thermal property enhancement can be achieved here using the phase change of water nanodroplets formed inside the water-in-FC-72 nanoemulsion fluids. In water-in-FC-72 nanoemulsion fluids, the fluid's heat capacity can be increased by the high specific heat of water(the volumetric heat capacity of water is about 4.18 J/ml K, and is over two times the heat capacity of PAO (1.74 J/ml K) [65]) and/or the latent heat of water is the highest among common heat transfer fluids (ΔH =334 J/g), depending on the operating

Figure 8. Relative Viscosity of Water-in-FC-72 Nanoemulsions versus volume fractions of water nanodroplets. The estimate from Einstein model is shown for comparison.

temperature of the fluids [66]. For example, the solid–liquid phase change of these droplets can increase the effective specific heat of the nanoemulsion fluid by a factor of $1 + \dfrac{\alpha \cdot H_{water}}{\Delta T \cdot C_{FC72}}$, where α is the water-volume fraction, H_{water} is the latent heat of fusion of water per unit volume, and ΔT is the temperature difference between the heat transfer surface and the bulk fluid.

The measured and calculated heat capacities of the water-in-FC-72 nanoemulsion fluids using a TA-CC100 DSC are shown in Figure 9. It can be seen that over 15 % increase in heat capacity can be achieved for a water volumetric fraction of 12 %, in which the measured $\alpha \cdot H_{water}$ values of the water-in-FC-72 nanoemulsions for water loadings of 3, 6, 9, and 12 vol. % are 10.52, 15.44, 25.48, 39.78 J/ml, respectively. The effective heat capacity of FC-72 can be enhanced by more than 200 % for a 12 vol.% of water-in-FC-72 nanoemulsion, according to these experimental data. It agrees well with theoretical prediction using the model mentioned above.

The use of phase-changeable nanodroplets (e.g. water nanodroplets) provides another way to simultaneously increase the effective specific heat and thermal conductivity of conventional heat-transfer fluids.

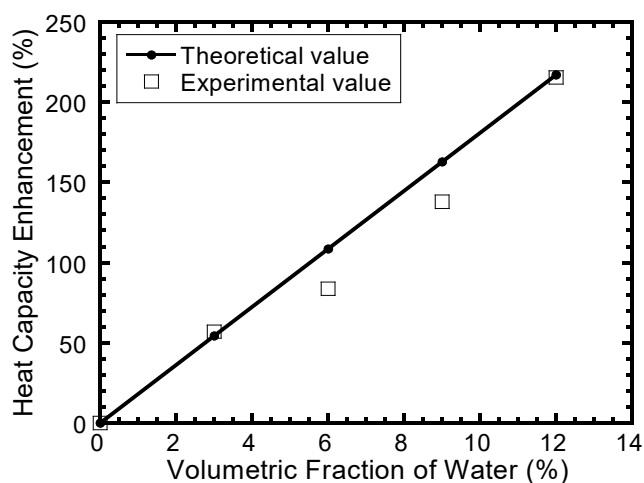### 3.3. Water-in-PAO nanoemulsion fluids

3.3.1. Microstructure of water-in-PAO nanoemulsion fluids

Figure 10 shows the SANS data for water-in-PAO nanoemulsion fluids with water volumetric concentration covering 1.8 vol. % to 10.3 vol.%.

It is clear from the SANS data that intensity curves of water-in-PAO nanoemulsion fluids gradually change the shape with increasing water loading. They can be further classified into three ranges (marked using three different colors): the 1.8–4.5 vol. % water-in-PAO nanoemulsion fluids with a smooth and gradually increasing scattering intensity for low q range
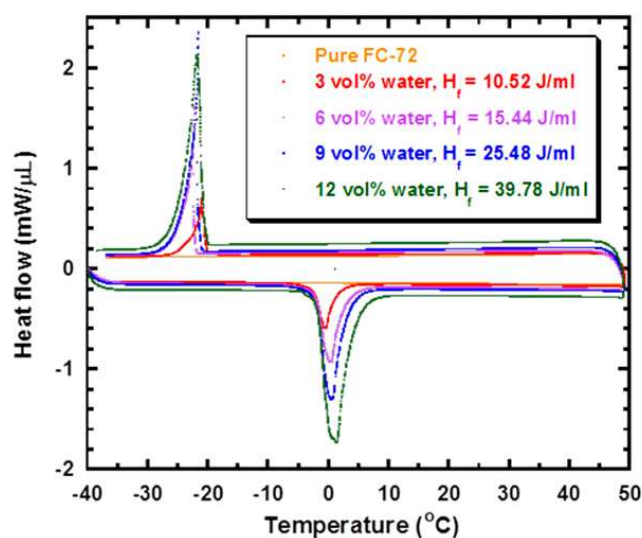
(a)

(b)

Figure 9. (a) DSC curves and latent heat of fusion values of water of the water-in-FC-72 nanoemulsion fluids with different water loadings. (b) The measured and calculated heat capacity enhancement in the water-in-FC-72 nanoemulsion fluids when the dispersed water droplets undergo solid–liquid phase transition.

(less than 0.1 Å); the 5.3–7.8 vol. % water-in-PAO nanoemulsion fluids with a sharper increase of q for the high q range (larger than 0.1 Å) and a flatter intensity curve for low q (less than 0.03 Å); and for even higher concentrations like 8.6 and 10.3 vol. % water-in-PAO nanoemulsion fluids tested here, the "hump" for high q is even more obvious and the intensity for low q increases more sharply which appears to have scattering curves made of three different sections. It indicates there is a dramatic microstructural change inside the water-in-PAO nanoemulsions of different water concentrations. Simple correlation length model cannot fit all the SANS curves well for both low and high q regions, as shown in Figure 11.

The hard sphere model (one typical simple correlation length model) fits well for low water concentrations (i.e. 1.8 % to 4.5 % volume fractions), and nanodroplet radii are found to be 13.2
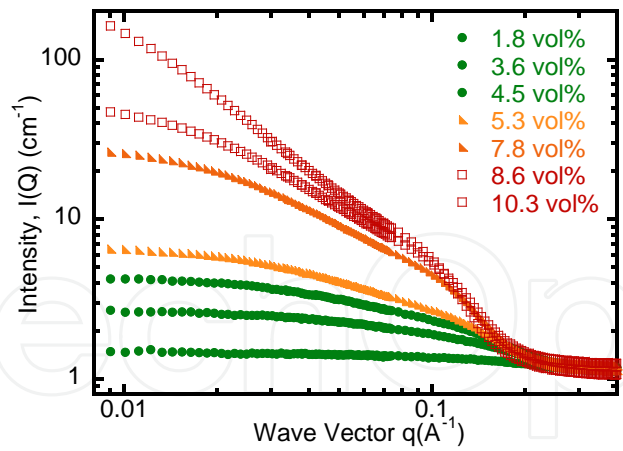
Figure 10. SANS curves for water-in-PAO nanoemulsion fluids for water volume concentration from 1.8 % to 10.3 %. Statistical error bars are smaller than the plotting symbols.
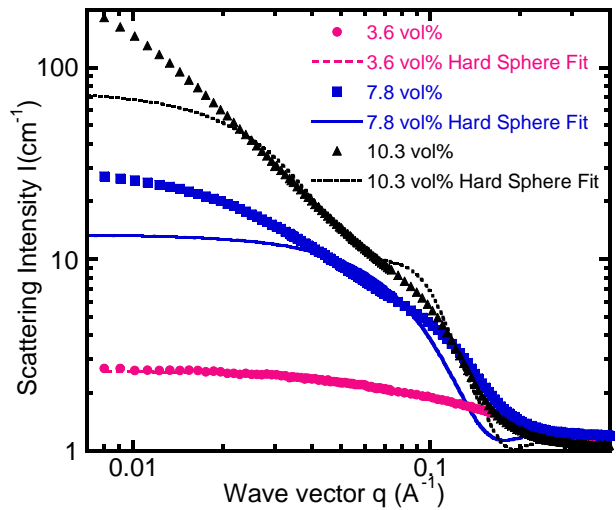
Figure 11. Small-angle neutron scattering curves for water-in-PAO nanoemulsion fluids (solid symbols) and hard sphere model curve fittings (colored lines).

Å, 25.6 Å, and 96 Å for water loading 1.8 vol. %, 3.6 vol. %, and 4.5 vol. %, respectively. For higher water concentration (i.e. 7.8 vol. % to 10.3 vol.%), the hard-sphere model does not fit well especially for scattering variable q less than 0.1 Å region, which suggests that those nanodroplets are not simply spherical.

Thus, a more comprehensive fitting model must be used to take into account of the structure change inside the water-in-PAO nanoemulsion fluids. Here, the three-region Guinier–Porod empirical model is used to accommodate the structural changes inside the system by fitting curves that are shown in Figure 12 [51, 54, 56, 68].

Generally, the scattering intensity is given by two contributions in the Guinier–Porod model:

$$I(Q) = \frac{G_2}{Q^{s_2}} \exp(\frac{-Q^2 R_{g2}^2}{3 - s_2}) \text{ for } Q \leq Q_2$$

$$I(Q) = \frac{G_1}{Q^{s_1}} \exp(\frac{-Q^2 R_{g1}^2}{3 - s_1}) \text{ for } Q_2 \leq Q \leq Q_1 \tag{5}$$

$$I(Q) = \frac{D}{Q^d} \text{ for } Q \geq Q_1$$

Here $3-s_1$ and $3-s_2$ are the dimensionality parameters, and R_{g1} and R_{g2} are the radii of gyration for the short and overall size of the scattering object. This generalized Guinier–Porod model can be used to analyze SANS patterns for nonspherical objects. In general, for scattering objects with spherical symmetry $s_1=s_2=0$ and for cylindrical objects $s_2=0$ and $s_1=1$. For lamellae with equal width and length, one has $s_2=0$ and $s_1=2$.
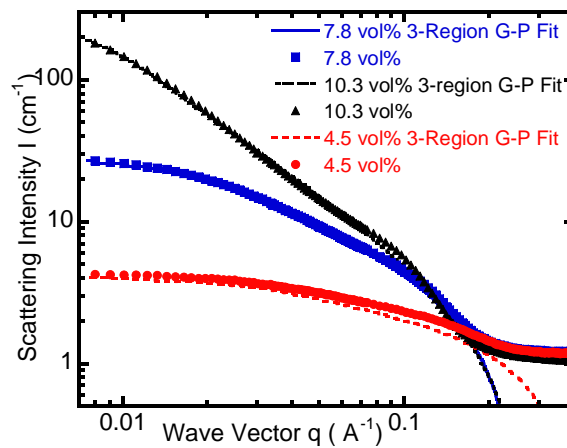

Figure 12. Small-angle neutron scattering curves for water-in-PAO nanoemulsion fluids (solid symbols) and three-region Guinier–Porod model curve fittings (colored lines).

Based on the fitting curves using the three-region Guinier–Porod model, there are two dimensionality parameters s_1 and s_2, plus R_{g2} and R_{g1} are the radii of gyration for the short and overall sizes of the scattering object. The fitted curves give $s_2=0.22$, $s_1=1.4$ and $R_{g2}=121$Å, $R_{g1}=4.6$Å for 10.3 vol. % water-in-PAO nanoemulsion fluids. For 7.8 % volume fraction water-in-PAO nanoemulsion fluid, $s_2=0.18$, $s_1=0.97$ and $R_{g2}=47.4$Å, $R_{g1}=5.2$Å. The dimensionality parameters suggest that those nanodroplets have a cylinder-like shape. So the SANS data confirm that there is an inner-structure variation with increasing water loading inside water-in-PAO nanoemulsion fluids. It is also noteworthy that the $s_2=0.04$ and $s_1=0.25$ is calculated for the 4.5 vol. % water-in-PAO nanoemulsion fluid and they can be approximated to $s_2 \approx 0$ and $s_1 \approx 0$, which agrees well with the interpretation of being spherical shape based on Hard Sphere model fitting. Note that for cylindrical droplets $R_{g2}^2 = \frac{L^2}{12} + \frac{R^2}{2}$, where L is the cylinder length and R is its radius and $R_{g1}^2 = \frac{R^2}{2}$.

3.3.2. Thermal conductivity of water-in-PAO nanoemulsion fluids

Figure 13 shows the thermal conductivity enhancement in water-in-PAO nanoemulsion fluids as a function of the loading of water from 0.47 % to 8.6 vol. %, in which the thermal conductivity linearly increases with higher water volume fraction and reaches a maximum of 16 % increase at 8.6 vol. % water.
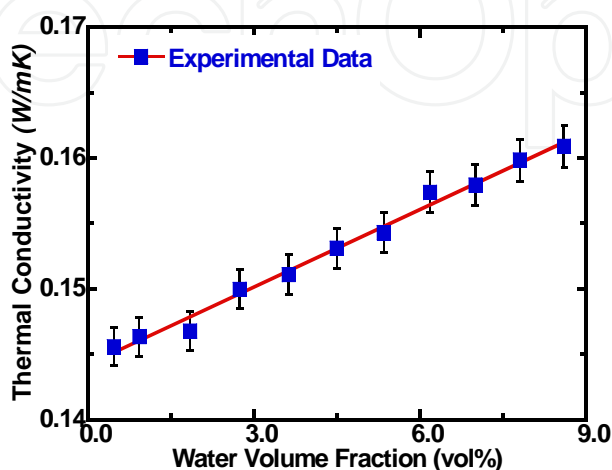

Figure 13. Thermal conductivity of water-in-PAO nanoemulsion fluids versus water volume fraction. The linear curve fit is shown for comparison.

3.3.3. Viscosity of water-in-PAO nanoemulsion fluids

The dynamic viscosity of water-in-PAO nanoemulsion fluids with different water volumetric concentrations is shown in Figure 14. All the water-in-PAO nanoemulsion fluids exhibit a shear-independent characteristic of Newtonian fluids. One unique phenomenon that can be seen in Figure 14 is that there is a maximum value in viscosity: it first increases with water concentration, reaches a maximum at 5.3 vol. %, and then decreases. This trend is different from the thermal conductivity shown in Figure 13 and the viscosity trend as observed in other nanoemulsion fluid systems. The maximum in viscosity can be attributed to the attraction force between droplets within the nanoemulsion fluids. The surfactant molecules become hydrated when more water is added inside and their counter ions are released into water which makes surfactants molecules and droplets charged oppositely so that the interdroplet attraction keeps increasing until the hydration process is complete. This may lead to a maximum viscosity in water-in-PAO nanoemulsion fluids as shown in Figure 14. It also coincides with the nonlinear inner structure change with increasing water concentration as seen in Figure 10.

### 3.3.4. Effective heat capacity of water-in-PAO nanoemulsion fluids

Similarly, the heat capacity of water-in-PAO nanoemulsion fluids was also investigated (shown in Figure 15). As shown in water-in-FC-72 nanoemulsion fluids, the water inside the water-in-PAO nanoemulsion fluids can increase the system's effective heat capacity through
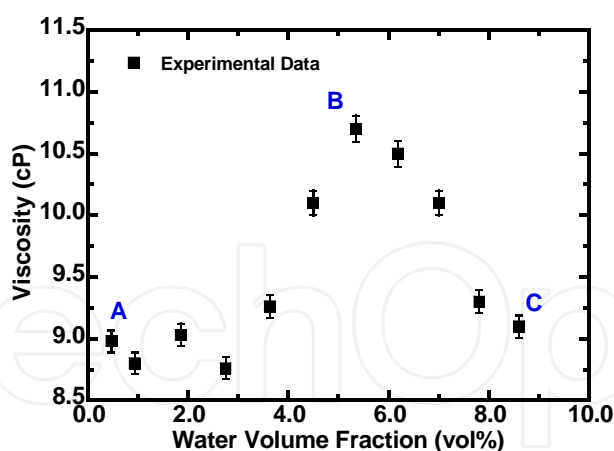
Figure 14. Dynamic viscosity of water-in-PAO nanoemulsion fluids versus volume fraction of water.

the high specific heat of water (i.e. C_{water}=4.2 J/g C, C_{PAO}=1.88 J/g C) and/or the latent heat of water (ΔH =334 J/g), depending on the operating temperature of the fluids.

DSC cyclic curves of water-in-PAO nanoemulsion fluids under different water loadings are shown in Figure 15. During the heating and cooling cycles, water nanodroplets undergo a melting–freezing transition in the nanoemulsion fluids. Interestingly, the presence of a single freezing peak in Figure 15 indicates a correspondence of the structural change with increasing water concentration (or water to surfactant molar ratio) as observed in our previous SANS measurement result: there is no obvious melting/freezing peak for water concentrations less than 4.5 vol. %, while the exothermic crystallization peak starts at around −20 ℃ when water concentration is higher or equal to 4.5 vol. %. When the water concentration is increased further above 8.6 vol. %, the freezing peak shifts to effect lower supercooling and peak values.
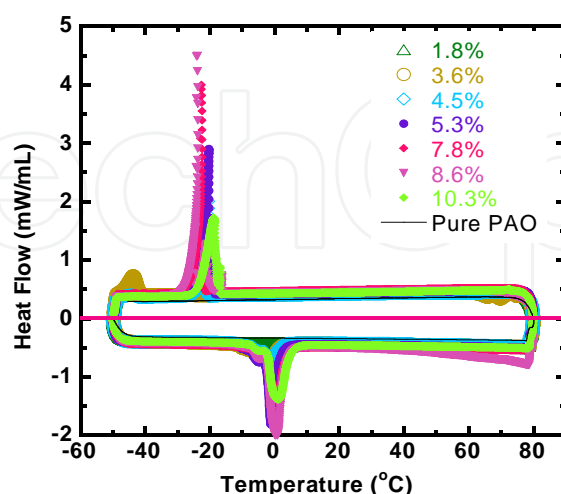
Figure 15. DSC cyclic curves of water-in-PAO nanoemulsion fluids for different water concentrations. Exothermal peaks are observed at −20 ℃, corresponding to the freezing of water nanodroplets, while endothermal peaks are observed at 0 ℃, corresponding to the melting of water nanodroplets.

To gain further insight into that, the specific heat of each sample is also calculated and summarized here in Table 2. The calculated H_f values of water-in-PAO nanoemulsions for different water concentrations from 5.3 to 8.6 vol. % are 17.7 and 28.724 J/g, respectively, in agreement with the measured results shown in Table 2, which are 26.72 J/g and 34.17 J/g, respectively. Based on the calculated values shown in Table 2, (1) the specific heat sharply increases from 9.8 J/g to 26.72 J/g when the water concentration is increased from 4.5 % to 5.3 vol. %; (2) the increase becomes moderate with higher water concentration; and (3) it decreases when the water concentration is higher than 8.6 vol. %. In addition to that, the freezing peak temperature is also decreased. All these occur to coincide with the structure transition with increasing water loading based on the SANS measurement.

Water % Fractions	Heat of Fusion (J/g)	Peak T (°C)
10.3	28.97	−18.88
8.6	34.17	−23.97
7.8	31.27	−22.74
5.3	26.72	−20.32
4.5	9.808	−20.63
3.6	2.48	-45
1.8	2.18	0

Table 2. Specific heat of water-in-PAO nanoemulsion fluids

In addition to that, a total maximum heat capacity increase of 88 % is obtained in the 8.6 vol. % water/PAO nanoemulsion fluids: for a temperature increase from −20 to 0 °C, 1 ml PAO absorbs 37.6 joules heat, and for the nanoemulsion containing 8.6 % water nanodroplets, the melting of ice nanoparticle absorbs 34 joules heat, it means that upon the melting of the ice nanoparticles in the nanoemulsion, the heat capacity of PAO has increased up by about 76 % in addition to the enhancement in heat capacity caused only by the addition of water without phase change (~12%).

4. Conclusions

The use of adding another material into thermal fluids has been emerged in recent years as a way to enhance the heat capacity and thermal conductivity of the base fluids simultaneously. A new type of nanostructured heat transfer fluids: nanoemulsion fluids are discussed in this chapter, such as ethanol-in-PAO, water-in-FC-72, and water-in-PAO nanoemulsion fluids. Many interesting properties have been reported in these nanoemulsion heat transfer fluids recently. The nanoemulsion heat transfer fluids can be formed by self-assembly and are thermodynamically stable. The self-assembled nanostructures have a significant effect on its macroscopic thermophysical properties which coincides with the structural characteristics

measured using SANS. In addition to that, the effective heat capacity of base fluid can also be greatly enhanced when those phase changeable nanodroplets undergo phase transition: the effective heat capacity of FC-72 by more than 200 % when those droplets undergo liquid–solid phase transition in water-in-FC-72 nanoemulsion fluids, and the effective heat capacity of PAO is increased by 80 % in water-in-PAO nanoemulsion fluids. The use of nanoemulsion fluids provides a means to increase the fluid conductivity and heat capacity simultaneously in the base fluids and their application in a wide variety of applications appears promising, but several critical issues remain to be solved in the future, for example, large subcooling or superheating during phase change due to lack of nucleation sites, and large viscosity increase due to the dispersed nanodroplets inside.

Acknowledgements

Author details

Bao Yang[2] and Jiajun Xu[1*]

*Address all correspondence to: jiajun.xu@udc.edu

1 Department of Mechanical Engineering, University of the District of Columbia, Washington DC, USA

2 Department of Mechanical Engineering, University of Maryland, College Park, MD, USA

References

[1] Eastman, J. A., Phillpot, S. R., Choi, S. U. S., and Keblinski, P., 2004, "Thermal transport in nanofluids," Annual Review of Materials Research, 34, pp. 219–246.

[2] Eastman, L. J., Choi, S. U. S., LI, S., and Thompson, L. J., 1997, "Enhanced thermal conductivity through development of nanofluids," Nanocrystalline and Nanocomposite Materials II.

[3] Inaba, H., 2000, "New challenge in advanced thermal energy transportation using functionally thermal fluids," International Journal of Thermal Sciences, 39(9–11), pp. 991–1003.

[4] Buongiorno, J., Venerus, D. C., Prabhat, N., McKrell, T., Townsend, J., Christianson, R., Tolmachev, Y. V., Keblinski, P., Hu, L.-W., Alvarado, J. L., Bang, I. C., Bishnoi, S. W., Bonetti, M., Botz, F., Cecere, A., Chang, Y., Chen, G., Chen, H., Chung, S. J., Chyu, M. K., Das, S. K., Di Paola, R., Ding, Y., Dubois, F., Dzido, G., Eapen, J., Escher, W., Funfschilling, D., Galand, Q., Gao, J., Gharagozloo, P. E., Goodson, K. E., Gutierrez, J. G., Hong, H., Horton, M., Hwang, K. S., Iorio, C. S., Jang, S. P., Jarzebski, A. B., Jiang, Y., Jin, L., Kabelac, S., Kamath, A., Kedzierski, M. A., Kieng, L. G., Kim, C., Kim, J.-H., Kim, S., Lee, S. H., Leong, K. C., Manna, I., Michel, B., Ni, R., Patel, H. E., Philip, J., Poulikakos, D., Reynaud, C., Savino, R., Singh, P. K., Song, P., Sundararajan, T., Timofeeva, E., Tritcak, T., Turanov, A. N., Van Vaerenbergh, S., Wen, D., Witharana, S., Yang, C., Yeh, W.-H., Zhao, X.-Z., and Zhou, S.-Q., 2009, "A benchmark study on the thermal conductivity of nanofluids," Journal of Applied Physics, 106(9).

[5] Zimparov, V., 2002, "Energy conservation through heat transfer enhancement techniques," International Journal of Energy Research, 26(7), pp. 675–696.

[6] Dewan, A., Mahanta, P., Raju, K. S., and Kumar, P. S., 2004, "Review of passive heat transfer augmentation techniques," Proceedings of the Institution of Mechanical Engineers Part A-Journal of Power and Energy, 218(A7), pp. 509–527.

[7] Boyd, R. D., 1985, "Subcooled flow boiling critical heat-flux (CHF) and its application to fusion energy components. 1. A review of fudamentals of CHF and related database," Fusion Technology, 7(1), pp. 7–30.

[8] Choi, S. U. S., Zhang, Z. G., Yu, W., Lockwood, F. E., and Grulke, E. A., 2001, "Anomalous thermal conductivity enhancement in nanotube suspensions," Applied Physics Letters, 79(14), pp. 2252–2254.

[9] Maxwell, J. C., 1904, "A treatise on electricity and magnetism," Oxford University Press, Cambridge, UK.

[10] Eastman, J. A., Choi, S. U. S., Li, S., Yu, W., and Thompson, L. J., 2001, "Anomalously increased effective thermal conductivities of ethylene glycol-based nanofluids containing copper nanoparticles," Applied Physics Letters, 78(6), pp. 718–720.

[11] Keblinski, P., Phillpot, S. R., Choi, S. U. S., and Eastman, J. A., 2002, "Mechanisms of heat flow in suspensions of nano-sized particles (nanofluids)," International Journal of Heat and Mass Transfer, 45(4), pp. 855–863.

[12] Prasher, R., Song, D., Wang, J. L., and Phelan, P., 2006, "Measurements of nanofluid viscosity and its implications for thermal applications," Applied Physics Letters, 89(13).

[13] Wang, X. Q., and Mujumdar, A. S., 2008, "A review on nanofluids - Part II: Experiments and applications," Brazilian Journal of Chemical Engineering, 25(4), pp. 631–648.

[14] Wang, X. Q., and Mujumdar, A. S., 2008, "A review on nanaofluids - Part I: Theoretical and numerical investigations," Brazilian Journal of Chemical Engineering, 25(4), pp. 613–630.

[15] Xu, J. J., Wu, C. W., and Yang, B., 2010, "Thermal- and phase-change characteristics of self-assembled ethanol/polyalphaolefin nanoemulsion fluids," Journal of Thermophysics and Heat Transfer, 24(1), pp. 208–211.

[16] Xu, J., Yang, B., and Hammouda, B., 2011, "Thermal conductivity and viscosity of self-assembled alcohol/polyalphaolefin nanoemulsion fluids," Nanoscale Research Letters, 6.

[17] Xu, J., Hammouda, B., and Yang, B., 2012, "Thermophysical properties and pool boiling characteristics of water in polyalphaolefin nanoemulsion fluids," ASME, Proceedings of ASME Micro/Nanoscale Heat & Mass Transfer International Conference 2012.

[18] Xu, J., and Yang, B., 2012, "Novel heat transfer fluids: Self-assembled nanoemulsion fluids," Nanotechnology, D. J. N. Govil, ed., Studium Press LLC.

[19] Yang, B., and Han, Z. H., 2006, "Thermal conductivity enhancement in water-in-FC72 nanoemulsion fluids," Applied Physics Letters, 88(26).

[20] Han, Z. H., Cao, F. Y., and Yang, B., 2008, "Synthesis and thermal characterization of phase-changeable indium/polyalphaolefin nanofluids," Applied Physics Letters, 92(24).

[21] Han, Z. H., and Yang, B., 2008, "Thermophysical characteristics of water-in-FC72 nanoemulsion fluids," Applied Physics Letters, 92(1).

[22] Han, Z. H., Yang, B., Qi, Y., and Cumings, J., 2011, "Synthesis of low-melting-point metallic nanoparticles with an ultrasonic nanoemulsion method," Ultrasonics, 51(4), pp. 485–488.

[23] Kumar, P., and Mittal, K. L., 1999, Handbook of microemulsion science and technology, New York: Marcel Dekker.

[24] Rosele, M. L., "Boiling of dilute emulsions," PhD Dissertation, University of Minnesota.

[25] Bulanov, N. V., Skripov, V. P., and Khmylnin, V. A., 1984, "Heat transfer to emulsion with superheating of its disperse phase," Journal of Engineering Physics, pp. 1–3.

[26] Bulanov, N. V., Skripov, V. P., and Khmylnin, V. A., 1993, "Heat transfer to tmulsion with a low-boiling disperse phase," Heat Transfer Research, pp. 786–789.

[27] Bulanov, N. V., 2001, "An analysis of the heat flux density under conditions of boiling internal phase of emulsion," High Temperature, 39(3), pp. 462–469.

[28] Bulanov, N. V., and Gasanov, B. M., 2005, "Experimental setup for studying the chain activation of low-temperature boiling sites in superheated liquid droplets," Colloid Journal, 67(5), pp. 531–536.

[29] Bulanov, N. V., Gasanov, B. M., and Turchaninova, E. A., 2006, "Results of experimental investigation of heat transfer with emulsions with low-boiling disperse phase," High Temperature, 44(2), pp. 267–282.

[30] Bulanov, N. V., and Gasanov, B. M., 2008, "Peculiarities of boiling of emulsions with a low-boiling disperse phase," International Journal of Heat and Mass Transfer, 51(7–8), pp. 1628–1632.

[31] Lunde, D. M., 2011, "Boiling dilute emulsions on a heated strip," MS thesis, University of Minnesota.

[32] Chen, S. J., Evans, D. F., and Ninham, B. W., 1984, "Properties and structure of 3-component ionic microemulsions," Journal of Physical Chemistry, 88(8), pp. 1631–1634.

[33] Ruckenstein, E., 1986, "The surface of tension, the natural radius, and the interfacial-tension in the thermodynamics of microemulsions," Journal of Colloid and Interface Science, 114(1), pp. 173–179.

[34] Siano, D. B., Bock, J., Myer, P., and Russel, W. B., 1987, "Thermodynamics and hydrodynamics of a nonionic microemulsion," Colloids and Surfaces, 26, pp. 171–190.

[35] Rosano, H. L., Cavallo, J. L., Chang, D. L., and Whittam, J. H., 1988, "Microemulsions - A commentary on their preparation," Journal of the Society of Cosmetic Chemists, 39(3), pp. 201–209.

[36] Chen, Z. Q., Chen, L. D., Hao, C., and Zhang, C. Z., 1990, "Thermodynamics of microemulsion. 1. The effect of alkyl chain-length of alkyl aromatics," Acta Chimica Sinica, 48(6), pp. 528–533.

[37] Moulik, S. P., Das, M. L., Bhattacharya, P. K., and Das, A. R., 1992, "Thermodynamics of microemulsion formation. 1. Enthalpy of solution of water in binary (triton-X 100 + butanol) and ternary (heptane + triton-X 100 + butanol) mixtures and heat-capacity of the resulting systems," Langmuir, 8(9), pp. 2135–2139.

[38] Moulik, S. P., and Ray, S., 1994, "Thermodynamics of clustering of droplets in water/AOT/heptane microemulsion," Pure and Applied Chemistry, 66(3), pp. 521–525.

[39] Ray, S., Bisal, S. R., and Moulik, S. P., 1994, "Thermodynamics of microemulsion formation. 2. Enthalpy of solution of water in binary-mixtures of aerosol-OT and heptane and heat-capacity of the resulting systems," Langmuir, 10(8), pp. 2507–2510.

[40] Strey, R., 1994, "Microemulsion and interfacial curvature," Colloid and Polymer Science, 272(8), pp. 1005–1019.

[41] Bergenholtz, J., Romagnoli, A. A., and Wagner, N. J., 1995, "Viscosity, microstructure, and interparticle potential of AOT/H$_2$O/N-decane inverse microemulsions," Langmuir, 11(5), pp. 1559–1570.

[42] Mukherjee, K., Mukherjee, D. C., and Moulik, S. P., 1997, "Thermodynamics of microemulsion formation. 3. Enthalpies of solution of water in chloroform as well as chloroform in water aided by cationic, anionic, and nonionic surfactants," Journal of Colloid and Interface Science, 187(2), pp. 327–333.

[43] Talegaonkar, S., Azeem, A., Ahmad, F. J., Khar, R. K., Pathan, S. A., and Khan, Z. I., 2008, "Microemulsions: a novel approach to enhanced drug delivery," Recent Patents on Drug Delivery & Formulation, 2(3), pp. 238–257.

[44] Wu, C., Cho, T. J., Xu, J., Lee, D., Yang, B., and Zachariah, M. R., 2010, "Effect of nanoparticle clustering on the effective thermal conductivity of concentrated silica colloids," Physical Review E, 81(1).

[45] Tyndall, J., 1868, "On the blue colour of the sky, the polarization of sky-light, and on the polarization of light by cloudy matter generally," Proceedings of the Royal Society of London, p. 223.

[46] He, G. S., Qin, H.-Y., and Zheng, Q., 2009, "Rayleigh, Mie, and Tyndall scatterings of polystyrene microspheres in water: Wavelength, size, and angle dependences," Journal of Applied Physics, 105(2).

[47] Haque, O., and Scamehorn, J. F., 1986, "Thermodynamics of microemulsion formation by mixtures of anionic and nonionic surfactants," Journal of Dispersion Science and Technology, 7(2), pp. 129–157.

[48] Mukhopadhyay, L., Mitra, N., Bhattacharya, P. K., and Moulik, S. P., 1997, "Thermodynamics of formation of biological microemulsion (with cinnamic alcohol, aerosol OT, Tween 20, and water) and kinetics of alkaline fading of crystal violet in them," Journal of Colloid and Interface Science, 186(1), pp. 1–8.

[49] De, M., Bhattacharya, S. C., Panda, A. K., and Moulik, S. P., 2009, "Interfacial behavior, structure, and thermodynamics of water in oil microemulsion formation in relation to the variation of surfactant head group and cosurfactant," Journal of Dispersion Science and Technology, 30(9), pp. 1262–1272.

[50] Moulik, S. P., and Paul, B. K., 1998, "Structure, dynamics and transport properties of microemulsions," Advances in Colloid and Interface Science, 78(2), pp. 99–195.

[51] Hammouda, B., Krueger, S., and Glinka, C. J., 1993, "Small-angle neutron-scattering at the national-institute-of-standards-and-technology," Journal of Research of the National Institute of Standards and Technology, 98(1), pp. 31–46.

[52] Chen, S. H., 1986, "Small-angle neutron-scattering studies of the structure and interaction in micellar and microemulsion systems," Annual Review of Physical Chemistry, 37, pp. 351–399.

[53] Gradzielski, M., and Langevin, D., 1996, "Small-angle neutron scattering experiments on microemulsion droplets: Relation to the bending elasticity of the amphiphilic film," Journal of Molecular Structure, 383(1–3), pp. 145–156.

[54] Hammouda, B., 2010, "SANS from polymers-review of the recent literature," Polymer Reviews, 50(1), pp. 14–39.

[55] Howe, A. M., Toprakcioglu, C., Dore, J. C., and Robinson, B. H., 1986, "Small-angle neutron-scattering studies of microemulsions stabilized by aerosel-OT. 3. The effect of addictives on phase-stability and droplet structure," Journal of the Chemical Society-Faraday Transactions I, 82, pp. 2411–2422.

[56] Marszalek, J., Pojman, J. A., and Page, K. A., 2008, "Neutron scattering study of the structural change induced by photopolymerization of AOT/D(2)O/sodecyl acrylate inverse microemulsions," Langmuir, 24(23), pp. 13694–13700.

[57] Nagao, M., Seto, H., Shibayama, M., and Yamada, N. L., 2003, "Small-angle neutron scattering study of droplet density dependence of the water-in-oil droplet structure in a ternary microemulsion," Journal of Applied Crystallography, 36, pp. 602–606.

[58] Wang, X.-Q., and Mujumdar, A. S., 2007, "Heat transfer characteristics of nanofluids: a review," International Journal of Thermal Sciences, 46(1), pp. 1–19.

[59] Wang, L. Q., and Wei, X. H., 2009, "Nanofluids: synthesis, heat conduction, and extension," Journal of Heat Transfer-Transactions of the Asme, 131(3).

[60] Ozerinc, S., Kakac, S., and Yazicioglu, A. G., 2010, "Enhanced thermal conductivity of nanofluids: a state-of-the-art review," Microfluidics and Nanofluidics, 8(2), pp. 145–170.

[61] Philip, J., and Shima, P. D., 2012, "Thermal properties of nanofluids," Advances in Colloid and Interface Science, 183, pp. 30–45.

[62] Cahill, D. G., 1990, "Thermal-conductivity measurement from 30-K to 750-K - The 3-omega method," Review of Scientific Instruments, 61(2), pp. 802–808.

[63] Yang, B., 2008, "Thermal conductivity equations based on Brownian motion in suspensions of nanoparticles (nanofluids)," Journal of Heat Transfer-Transactions of the Asme, 130(4).

[64] Touloukian, Y. S., Liley, P. E., and Saxena, S. C., 1970, "Thermal conductivity for non-metallic liquids & gases," Washiongton: IFI/PLENUM, Thermophysical Properties of Matters.

[65] 2002, "Synfluid PAO databook," Chveron Philips Chemical LP, *Synfluid PAO Databook*.

[66] 3M, "Fluorinert™ electronic liquid FC-72 product information."

[67] Evans, W., Fish, J., and Keblinski, P., 2006, "Role of Brownian motion hydrodynamics on nanofluid thermal conductivity," Applied Physics Letters, 88(9).

[68] Hammouda, B., 2010, "A new Guinier-Porod model," Journal of Applied Crystallography, 43, pp. 716–719.

[69] Mulligan, J. C., Colvin, D. P., and Bryant, Y. G., 1996, "Microencapsulated phase-change material suspensions for heat transfer in spacecraft thermal systems," Journal of Spacecraft and Rockets, 33(2), pp. 278–284.